Original article

A Novel Genus of Virulent Phage Targeting *Acinetobacter baumannii*: Efficacy and Safety in a Murine Model of Pulmonary Infection

JiaWang.Wang[a,b,c],Huan.Hu[b,c],QingQing.Wang[b,c],TianZhu.Zhu[b,c],XiaoHan.Ren[b,c],Wen Qian.Jiang[b,c],XueMei.Hou[b,c,*],Jun.Lin[b,c,*],XiaoLing.Yu[a,b,c,*]

a) Department of Pharmacy, Mengchao Hepatobiliary Hospital of Fujian Medical University, FuZhou 350025, China;

b) Institute of Applied Genomics, Fuzhou University, FuZhou 350108, China;

c) College of Biological Science and Engineering, Fuzhou University, FuZhou 350108, China;

* Corresponding author

Xiaoling.Yu: Department of Pharmacy, Mengchao Hepatobiliary Hospital of Fujian Medical University, Fuzhou, China; 350025;E-mail:xiaolingyu82@163.com;Tel: +86 591 88116019;

Jun.Lin: Institute of Applied Genomics, College of Biological Science and Engineering,Fuzhou University, Fuzhou, China;350108; E-mail: jun@fzu.edu.cn;Tel: +86 591 22863805;

XueMei.Hou: Institute of Applied Genomics, College of Biological Science and Engineering,Fuzhou University, Fuzhou, China;350108; E-mail: houxuemei_1990@163.com;Tel: +86 591 22863805;

Abstract

Acinetobacter baumannii (*A.baumannii*) is a notable opportunistic pathogen responsible for severe hospital-acquired infections, with multidrug-resistant strains posing significant treatment challenges. Phage therapy, which employs bacteriophages as natural bacterial antagonists, has gained renewed attention as a promising solution to combat antibiotic-resistant infections. In this study, we isolated and characterized a novel virulent phage, vB_AbaS_qsb1, which specifically lyses *A.baumannii*. Phylogenetic and genomic analyses indicate that vB_AbaS_qsb1 is the founding member of a previously unreported genus, which we have named as *Acinibactriovirus*, with *Acinibactriovirus lysinus* as the type species. vB_AbaS_qsb1 demonstrated robust stability across diverse temperature and pH ranges, a short latent period, and no known virulence or antibiotic resistance genes within its 54,713 bp dsDNA genome. Safety assessments showed that high-dose vB_AbaS_qsb1 induced no adverse effects in mice, with histopathology confirming its safety profile. Therapeutic experiments further indicated that vB_AbaS_qsb1 provided at least 50% protection against *A.baumannii*-induced pneumonia, significantly reducing bacterial loads and inflammation markers, while maintaining high phage titers in lung tissue.This study introduces vB_AbaS_qsb1 as a promising candidate for phage therapy against *A.baumannii*, offering both innovative insights and a valuable framework for future isolation, genomic characterization, and efficacy evaluation of phages targeting antibiotic-resistant bacteria.

Graphical abstract

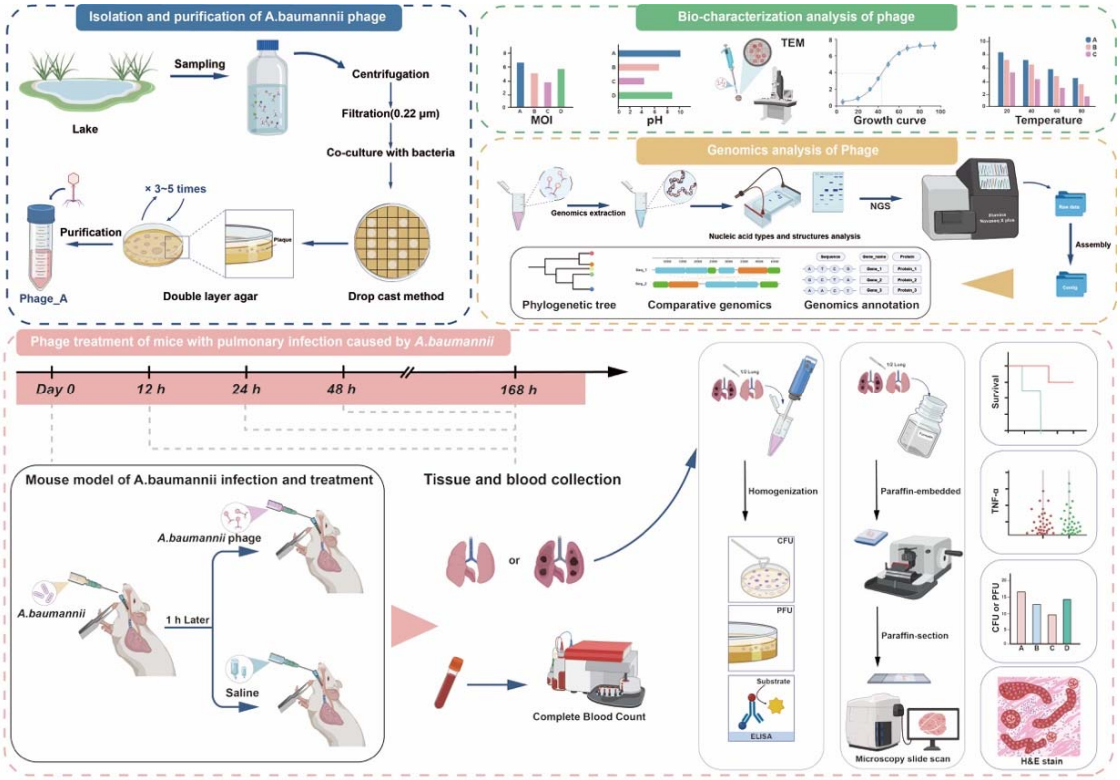

Key words

Acinetobacter baumannii, Phage therapy, Bacteriophage (or phage), Pulmonary infection, Mice, *In-vivo* therapy

Introduction

A.baumannii is a Gram-negative, non-motile opportunistic pathogen commonly found in aquatic and soil environments, and a leading cause of nosocomial infections. It is associated with high mortality rates, particularly in ICU settings where infections such as pneumonia and sepsis can result in mortality rates as high as 54%[1, 2]. This pathogen is a major contributor to lung infections, sepsis, meningitis, urinary tract infections, and wound infections[3].

In clinical practice, antibiotics are commonly used to treat *A.baumannii* infections, but the misuse of these drugs has led to the rise of multidrug-resistant (MDR) strains, including carbapenem-resistant *A.baumannii* [4]. While combination antibiotic therapy is employed to combat resistance[5], its effectiveness can be limited by antagonistic interactions and may even promote broad-spectrum resistance[6]. The high mortality rate of *A.baumannii* infections stems from its inherent resistance and ability to acquire resistance genes[7, 8]. In response, the WHO classified carbapenem-resistant *A.baumannii* as a critical priority for antibiotic development in 2017, reaffirming its importance in 2024[9, 10].

Given the escalating challenge of antibiotic resistance, the need for novel antimicrobial treatments is pressing. Phage therapy, an ancient yet increasingly promising approach, has garnered renewed interest. Bacteriophages are viruses that specifically infect bacteria, and based on their lifecycle, they can be categorized as either virulent or temperate[11]. Due to their ability to specifically lyse bacterial pathogens without harming eukaryotic cells, virulent phages have emerged as

potential therapeutic agents for treating bacterial infections[12]. In vitro studies have demonstrated the potent antibacterial activity of phages, showing their ability to effectively eliminate bacteria and disrupt biofilms[13]，Jeremy J. Barr *et al.*[14, 15] demonstrated that both single phage therapy and phage-antibiotic combination therapy can effectively alleviate infection symptoms in mice. Furthermore, *in vivo* studies of animals have confirmed the safety and efficacy of phage therapy in treating bacterial infections[16, 17]. Numerous compassionate-use cases have highlighted the clinical success of phage therapy in treating various infections, including lung infections[18, 19], pancreatic infections[20], osteomyelitis[21], and enteritis[22].In this study, we isolated and systematically characterized a novel virulent phage, vB_AbaS_qsb1, targeting *A.baumannii* from environmental sewage, with its biological properties and genomic features comprehensively detailed. Remarkably, phylogenetic analysis revealed that vB_AbaS_qsb1 belongs to a previously unreported genus, which we have named as *Acinibactriovirus*, with vB_AbaS_qsb1 serving as the type species (*Acinibactriovirus lysinus*). This classification underscores the novelty of our work, as it introduces a new genus of phages with significant potential for therapeutic applications against multidrug-resistant *A.baumannii*.The phage has been preserved in the Guangdong Microbial Culture Collection Center (GDMCC, accession number GMDCC 64831-B1). Additionally, we developed a mouse model of *A.baumannii*-induced pneumonia to evaluate both the safety and antibacterial efficacy of vB_AbaS_qsb1 in vivo. This model is essential for assessing the phage's ability to reduce bacterial loads, enhance survival rates, and confirm its

safety profile, providing a robust foundation for potential clinical applications in combating resistant *A.baumannii* infections.

Result

Purification and morphology of a novo-bacteriophage vB_AbaS_qsb1

A potent *A.baumannii* phage, vB_AbaS_qsb1, was successfully isolated from local lake(QiShan lake, FuZhou city, FuJian provience, China) water sample, utilizing *A.baumannii* strain *ioag01* as the host. Following preprepared double-layer agar plates seeded with qsb1 and *ioag01*, and subsequent incubation at 37□ overnight, distinct plaques with an average diameter of approximately 4.0±1.0 mm were observed, accompanied by a depolymerase halos with an approximate measurement of 7.0±1.0 mm (Figure 1A).Transmission electron microscopy (TEM) analysis (Figure 1B) revealed that the phage's head dimensiona were approximately 70×80 nm, with a tail extending about 90 nm in length and a tail diameter of 20 nm. In accordance with the International Committee on Taxonomy of Viruses (ICTV) classification and nomenclature criteria, the phage was designated as vB_AbaS_qsb1. The phage has been archived in the Guangdong Microbial Culture Collection Center (GDMCC) with the accession number GMDCC 64831-B1.

The study of the biological characteristics of qsb1 showed that the optimal phage replication efficiency was achieved at an multiplicity of infection (MOI) of 0.1 (Figure 1C). At this MOI, phage proliferation exhibited a two-log increase within 6 hours under these conditions. The one-step growth curve of qsb1 revealed a short

latent period (about 20 minutes), followed by an exponential phase(about 100 minutes), with a burst size of approximately 23 plaque-forming units (PFU) /cell (Figure 1D).Thermal stability analysis demonstrated that qsb1 remains stable between 10 □ and 60 □, though the phage lost all activity at 80 □ and 100 □ (Figure 1E). pH stability testing indicated qsb1 stability across a pH range of 3 to 11, with significant reductions in activity observed at pH 1 and complete inactivation at pH 13 (Figure 1F). Overall, qsb1 shows robust stability under normal physiological conditions, with activity only compromised under extreme heat or pH levels.

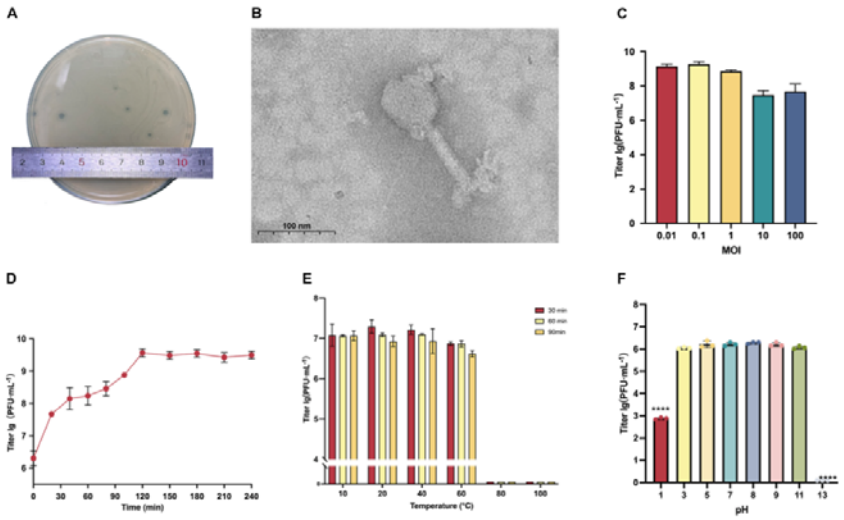

Figure 1: Biological Characteristics of Bacteriophage vB_AbaS_qsb1

(A) Plaque morphology of vB_AbaS_qsb1 on double-layer agar plates. When vB_AbaS_qsb1 and *ioag01* were co-cultured in soft agar overnight at 37□, clear transparent plaques and distinct depolymerase halos were observed.

(B) Transmission electron microscopy (TEM) image of vB_AbaS_qsb1 morphology, negatively stained with 4% phosphotungstic acid, The scale bar corresponds to 100 nm.

(C) MOI of vB_AbaS_qsb1, showing phage titer following infection of its host at various MOIs.

(D) One-step growth curve of vB_AbaS_qsb1.

(E) Temperature stability of vB_AbaS_qsb1, represented by titer variations at different temperatures across varying time periods.

(F) pH stability of vB_AbaS_qsb1. All samples were analyzed in triplicate, and the results are expressed as mean values ±SD.

Genome characteristics of the phage vB_AbaS_qsb1

Genome features of phage vB_AbaS_qsb1

Pulsed-field gel electrophoresis (PFGE) estimated the genome size of vB_AbaS_qsb1 to be approximately 50 kbp (Supplementary Figure S1). Next-generation sequencing (NGS) revealed that the qsb1 genome comprises 54,713 base pairs (Figure 2) of double-stranded DNA (verified using RNAse A, DNAse I and S1 nuclease; Supplementary Figure S2 and S3), with a GC content of 39%. A total of 95 coding DNA sequences (CDSs) were identified, numbered from CDS_1 to CDS_95 (Supplementary Table S1). Among these, 42 CDSs were predicted to encode proteins with known functions, while the remaining 51 were classified as hypothetical proteins with uncharacterized roles. The identified proteins are involved in key biological processes such as structural assembly, DNA replication and repair, gene regulation, host recognition, and infection mechanisms. Notably, an integrase gene (CDS_1), typically associated with lysogeny, was identified, but experimental data and lifestyle prediction analyses confirmed that qsb1 functions as a virulent phage in both in vivo and in vitro studies. Additionally, the genome encodes a lysozyme (CDS_6), likely

enhancing the phage's ability to degrade extracellular polysaccharides, aiding in bacterial lysis and biofilm disruption. Comprehensive scans using CRAD and Phagescope did not detect any virulence or antibiotic resistance genes, indicating that qsb1 is a promising and safe candidate for phage therapy. (The NGS raw sequencing data have been deposited in the SRA databases, SRA data accession: PRJNA1170883)

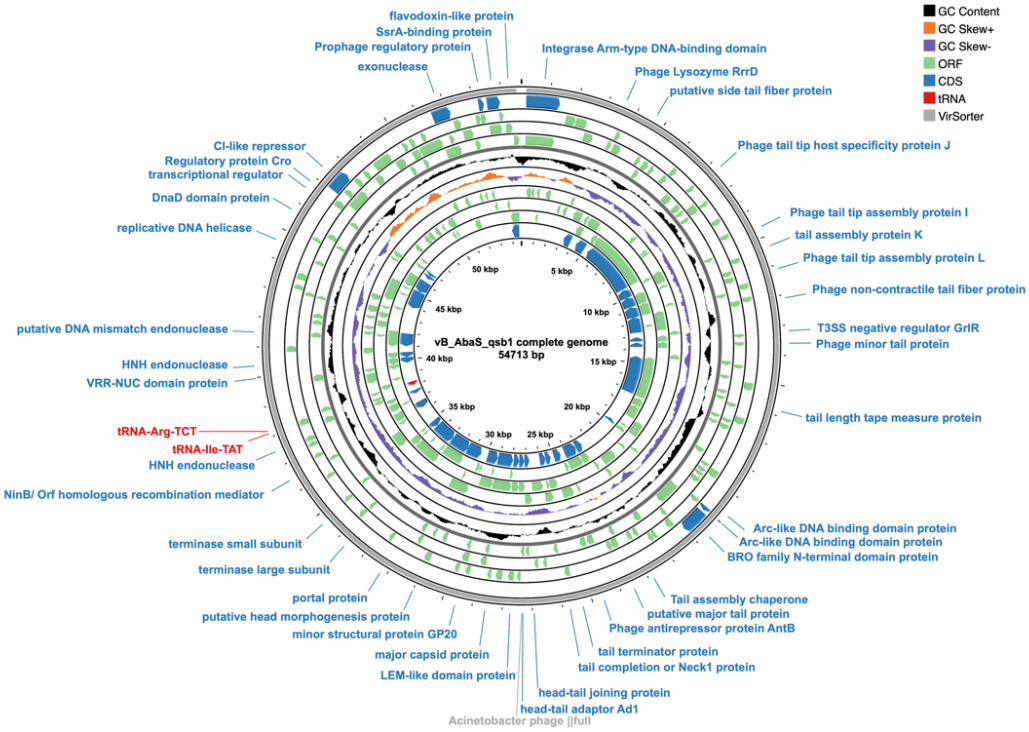

Figure 2: Whole-Genome Circular Map of Bacteriophage vB_AbaS_qsb1. The black ring represents the GC content, while the orange and purple rings display the CG skew for the positive and negative strands, respectively. Green rings denote predicted open reading frames (ORFs), and blue rings correspond to coding sequences (CDSs) annotated with predicted protein functions. Red labels indicate tRNAs, and grey highlights identifiable viral sequences. Pseudogenes or proteins of unknown function are excluded from the map.

Phylogenetic Analysis

To elucidate the phylogenetic background of bacteriophage vB_AbaS_qsb1, we

performed a BLAST search against all viral genome databases in the NCBI repository, identifying a total of 88 sequences. Among the BLAST results, phages from the genera *Vieuvirus*, *Obolenskvirus*, and unclassified members of the family *Caudoviricetes* were detected.

We compared all previously reported complete *Acinetobacter* phage genome sequences (74 in total) and noted that the remaining 14 phages with partial genomes displayed coverage rates ranging from 0% to 49% (Supplementary Table S2). This analysis revealed that vB_AbaS_qsb1 is closely related to *Acinetobacter* phage vB_AbaS_TRS1 and MAG_*Caudoviricetessp* _Isolate_224 (Figure 3A), with both clustering in the same cluster, and indicating genus-level consistency. However, the results of colinearity comparison showed that the genomes of vB_AbaS_qsb1, vB_AbaS_TRS1 and Isolate_224 were extremely different (Figure 3B), and the coverage of vB_AbaS_qsb1 on vB_AbaS_TRS1 and Isolate_224 was extremely low (only 20% and 2%, respectively). Furthermore, NCBI records indicate that neither VB_AbaS_TRS1 nor Isolate_224 has been formally classified within a recognized genus. Therefore, we suggested that vB_AbaS_qsb1 is also a phage independent of any known genus.

Further phylogenetic comparisons were made between qsb1 and representative members of the genera Vieuvirus and Obolenskvirus in both AAI and GBDP analyses. The AAI values for Vieuvirus phages ranged from 58.65% to 73.07%, while those for Obolenskvirus phages ranged from 32.15% to 62.75% (Supplementary Tables S3 and S4). According to ICTV standards, AAI values between 75% and 95% indicate

distinct species within the same genus. Thus, the observed AAI and GBDP results support the classification of qsb1 as a distinct species within a novel phage genus.

Similarly, average nucleotide identity (ANI) analysis showed that the OrthoANIu values between qsb1 and representative phages YMC11_11_R3177 and AP22 were only 73.50% and 73.40%, respectively, further supporting its distinction from known species and genera (Supplementary Table S5).

The combined AAI, ANI, GBDP, and synteny analyses strongly suggest that qsb1 represents a novel genus, named *Acinibactriovirus*, and a novel species, *Acinibactriovirus lysinus*, within the *Acinetobacter* phage lineage. These results underscore the unique genomic characteristics of qsb1 and open avenues for further taxonomic and functional exploration.

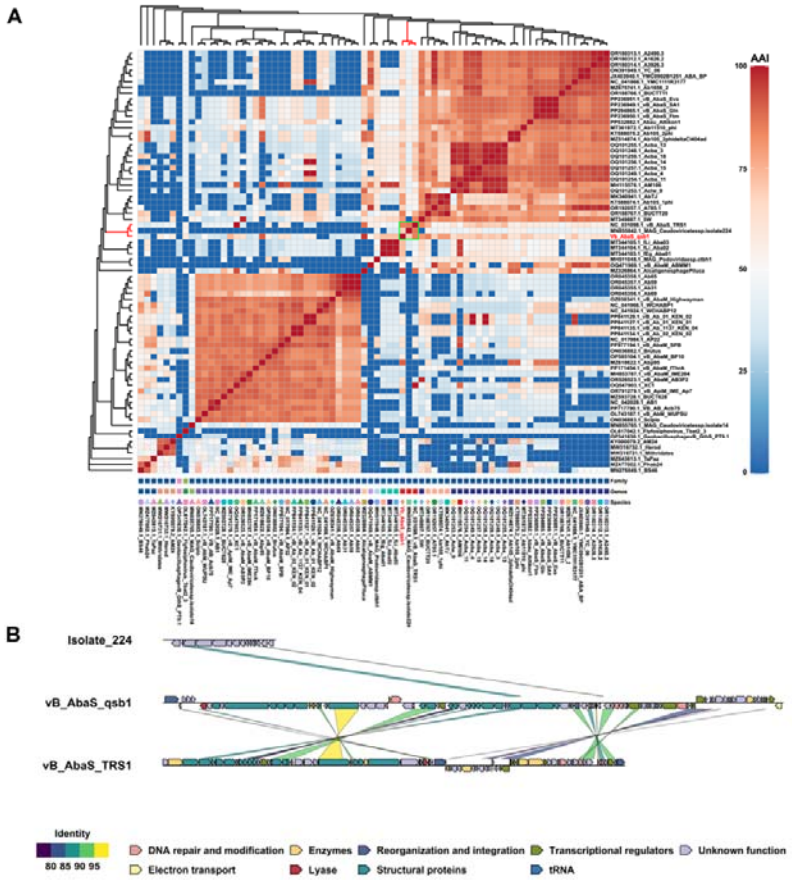

Figure 3: Heat map of complete genome analysis and Collinearity Analysis

(A) Heat map of AAI (Average Amino Acid Identity) values and Genome BLAST Distance Phylogeny (GBDP) analysis for 74 complete *Acinetobacter* phage genomes. The AAI values range from 0% (blue) to 100% (red), depicting the degree of genetic similarity among phages. The evolutionary tree on the left and top represents GBDP analysis, showing the phylogenetic relationships among 74 phages. Symbols and colors at the bottom correspond to taxonomic differences at the family, genus, or species level. Vertical axis labels represent the family, genus, or species, with matching shapes and colors indicating consistency at specific taxonomic levels.

(B) Collinearity comparison of the vB_AbaS_qsb1 genome with vB_AbaS_TRS1 and Isolate_224. Arrows indicate the location and orientation of CDSs in each genome (right-pointing arrows for the positive strand, left-pointing arrows for the negative strand). The lines between genomes illustrate sequence similarities (as represented in the bottom left corner) , and CDSs are color-coded by functional categories, as shown in the legend in the bottom right corner.

Phage therapy for acute pulmonary infection caused by *A.baumannii* in mice

Establishment of the model of pulmonary infection caused by *A.baumannii* in mice

A BALB/C mouse model of acute pulmonary infection caused by *A.baumannii* was established by tracheal instillation of bacteria directly into the trachea.

Over the course of a 7-day observation period, all mice in the 3×10□ Colony-forming units (CFU)/mouse group died within 36 hours, and those in the 3×10□ CFU/mouse group had a mortality rate of 83.3%. In contrast, only one mouse in the 3×10□

CFU/mouse group succumbed (a mortality rate of 16.7%), and no mortality was observed in either the 3×10□ CFU/mouse group or the control group (Figure 4A). Based on the median lethal dose (LD□□) criteria and to ensure the study's comparability, a bacterial dose of 3×10□ CFU/mouse was selected for subsequent experiments to construct a reliable model of pulmonary infection in mice.

The Safety of phage therapy

To assess whether *A.baumannii* phage qsb1 induces severe immune responses or adverse clinical symptoms in mice, phage preparation was instilled into the lungs. Throughout the 7-day observation period, none of the mice in the phage-treated group exhibited any negative clinical symptoms, and no deaths occurred (Figure 4A). Whole blood samples of mice were collected for complete blood count（CBC）. The results indicated no significant differences in the levels of white blood cells and neutrophils between the phage-treated group and the control group (Figure 4B). Analysis of relative inflammatory cytokine levels (TNF-α, IL-6, and IL-1β) in mouse lung tissue (Figure 4C) indicated that phage treatment did not trigger a severe immune response in mice. Furthermore, hematoxylin-eosin (HE) staining analysis (Figure 4D) revealed no significant infiltration of inflammatory cells in the lung tissue, no apparent congestion, and the alveolar structure remained intact. Summary, no severe immune responses or lung tissue damage were observed in mice treated with phage qsb1, confirming its safety.

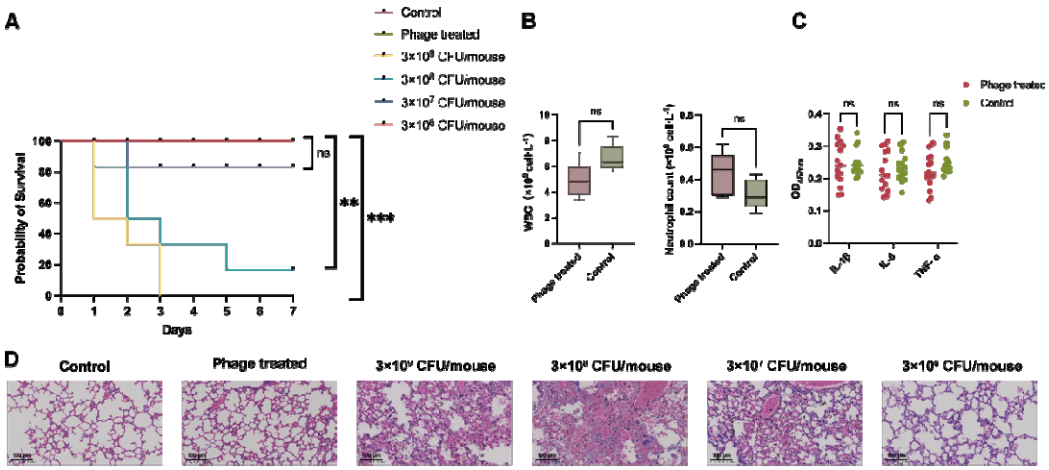

Figure 4: Mouse model of *A.baumannii* lung infection and phage safety evaluation. The control group received saline treatment only, while the phage-treated group received 10□ PFU of qsb1. Other groups were administered varying doses of *A.baumannii* culture.

(A) Survival curve of mice during the 7-day observation period (n=6 for the Control, 3×10^9 CFU/mouse, 3×10^8 CFU/mouse, 3×10^7 CFU/mouse and 3×10^6 CFU/mouse, n=5 for the Phage treated group).

(B) Leukocyte and neutrophil counts in whole blood of the control and phage treated groups (n=5). The results indicate no significant differences in leukocyte and neutrophil levels between the phage-treated and control groups.

(C) Relative levels of inflammatory cytokines (IL-1β, IL-6, and TNF-α) in mouse lung tissues (n=5). The data demonstrate no significant differences in the levels of IL-1β, IL-6, and TNF-α between the phage-treated and control groups.

(D) Pathological examination of mouse lung tissue. Scale bar=100μm. Statistical analysis of survival curves was performed using the log-rank test, while other data were analyzed using two-way ANOVA. ***$p < 0.001$, **$p < 0.01$, *$p < 0.05$.

Phage treatment of mice with pulmonary infection caused by *A.baumannii*

To investigate the efficacy of different phage doses on the treatment of pneumonia-infected mice, phage therapy was administered 1 hour post-infection. In the Mock-treated group, a substantial number of mice (4/5) succumbed within 48 hours, resulting in a final survival rate of 20%. Similarly, in both the Medium-dose and Low-dose phage treated groups, most mice died (4/5) within 96 hours, with a survival rate of 20% by day 7. The survival rates in these groups were significantly lower than those observed in the control group. Remarkably, in the High-dose phage treated group, only one mouse died(1/5) following phage treatment, and the survival rate reached 80%, which was not significantly different from that of the control group (Figure 5A).

After the 7-day observation period, the mice were sacrificed, and blood samples were collected for CBC. The results showed no significant differences in leukocyte and neutrophil counts between the high-dose phage-treated group and the control group (Figure 5B). Histopathological examination of lung tissues with hematoxylin-eosin (HE) staining revealed substantial damage to the alveolar structure in the Mock, Medium-dose, and Low-dose treated groups, including a marked reduction in normal alveoli, inflammatory exudates in the alveolar spaces, thickened and ruptured alveolar septa, and significant congestion and necrosis of lung tissue. In contrast, the high-dose treated group displayed well-preserved lung architecture, with intact alveoli and no evident pathological changes, closely resembling the control group's lung morphology (Figure 5C). In summary, high-dose phage therapy significantly enhances the survival rate of infected mice and effectively prevents the development of lung lesions.

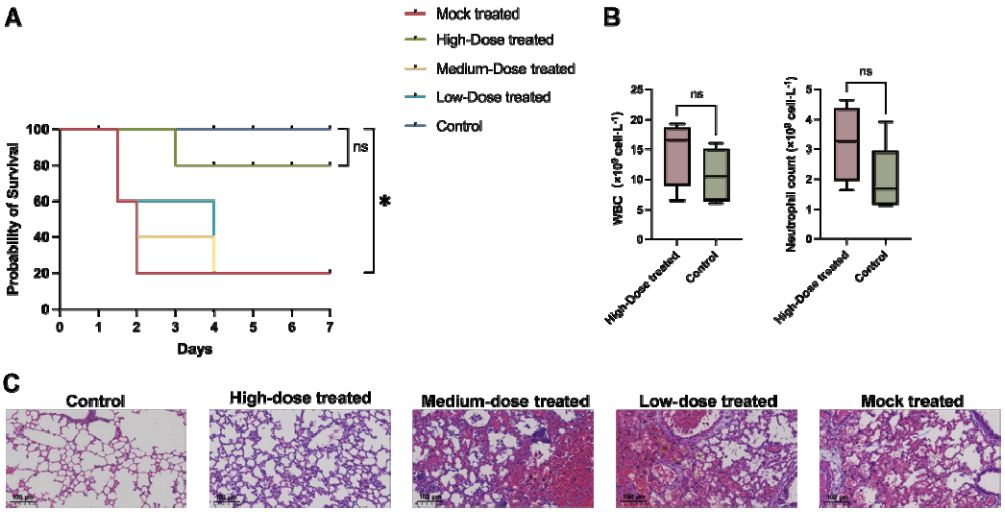

Figure 5: Phage therapy in lung-infected mice via tracheal instillation. The control group received only saline without infection, while the Mock-treated group was administered 3×10□ CFU of *A.baumannii ioag01* without any treatment. Mice in the high, medium, and low-dose phage treatment groups were administered 3×10□, 3×10□, and 3×10□ PFU of qsb1, respectively, following infection.

(A) Survival curve of mice over 7 days following treatment with different doses of phage (n=5).

(B) White blood cell and neutrophil counts in mice 7 days post high-dose phage treatment (n=4).

(C) Histopathological examination of lung tissue after phage treatment; scale bar = 100 μm. Survival curves were analyzed using the log-rank test, and other data were analyzed using two-way ANOVA. ***$p < 0.001$, **$p < 0.01$, *$p < 0.05$.

Dynamic changes in infection status of mice during phage treatment

As previously established, a phage dose of 3×10□ PFU/mouse demonstrated substantial efficacy against lung infection. To further investigate the dynamic progression of the disease during treatment, phages were administered 1 hour post-infection, and 6 mice from each experimental group were euthanized at various

time points after infection (12 h, 24 h, 48 h, and 168 h) to collect blood and lung tissue.

Over the 7-day observation period, all mice in the mock-treated group succumbed within 60 hours (Figure 6A). However, 50% of the mice in the phage-treated group survived by the end of the observation period (168 hours). These findings align with our previous studies, demonstrating that phage qsb1 therapy can significantly improve survival rates in mice suffering from acute pneumonia infected by *A.baumannii*. CBC results (Figure 6B) indicated a continuous rise in white blood cell counts over the first 48 hours, suggesting the progression of inflammation. besides, the TNF-α levels in the phage-treated group were significantly lower than those in the model control group (Figure 6E). These findings indicate that phage treatment effectively mitigated the inflammatory response in the lungs.

The results of lung homogenate colony counts showed that, The bacterial colonization in the lungs of mice in the mock treatment group remained at a high level(10□ to 10^{1}□ CFU/g) (Figure 6C). In contrast, bacterial colonization in the phage-treated group was significantly lower at all time points. By the 48-hour mark, bacterial colonization in the phage-treated group had decreased to just 10^{6} CFU/g.

Additionally, the phage titer in the lungs of the Phage-treated group was monitored during infection (Figure 6D). At 12 hours after infection, the phage titer was 10□ PFU/g. Over time, the phage titer steadily increased, corresponding with bacterial colonization, as the phages continued to infect and alleviate infection symptoms. By 168 hours, the phage titer had reached 10^{1}□ PFU/g, indicating continuous phage

activity in combating infection and without being cleared by the immune system.

Finally, histopathological examination of lung tissue (Figure 6F) revealed that , as the infection progressed, severe lung damage became apparent, including congestion, necrosis, inflammatory cytokine infiltration, and extensive destruction of the alveolar structure. In the Phage-treated group, only minor alveolar edema and limited inflammatory infiltration were observed at all time points, with alveolar structures remaining largely intact, and no signs of congestion, necrosis, or other severe pathological changes.

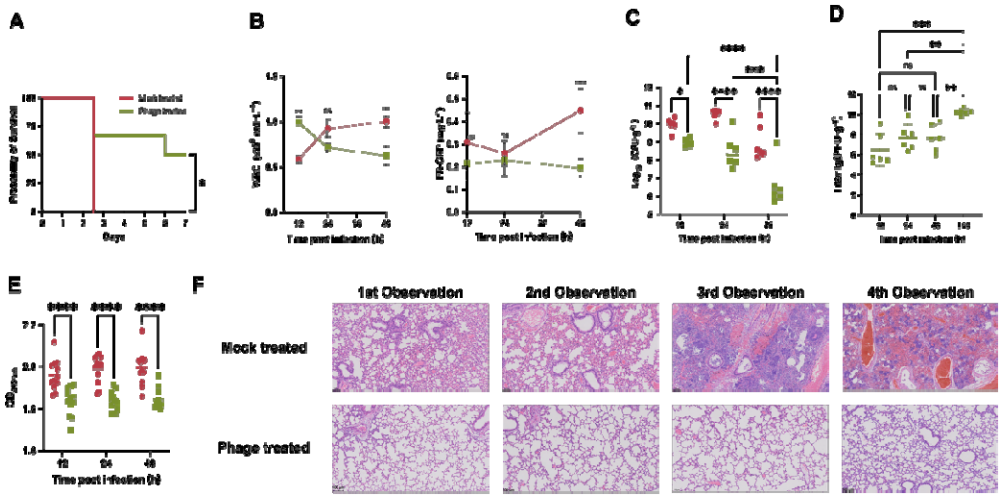

Figure 5: High-dose phage treatment in mice with *A.baumannii* lung infection.

Saline (red circles) and qsb1 phage (green squares) were administered 1 hour post-infection with *A.baumannii*. The 1st, 2nd, and 3rd observations correspond to 12h, 24h, and 48h, respectively. The 4th observation is at 60h for the Mock treated group (all mice died by 60h) and 128h for the Phage treated group.

(A) Seven-day survival curve for mice after high-dose phage treatment (n=6): Mock-treated group (red) and Phage-treated group (green). The survival rate (50%) in the phage-treated group was

significantly higher than that in the Mock-treated group at the end of treatment.

(B) Changes in blood cell counts (WBC and CRP) over the course of treatment (n=6).

(C) Bacterial CFU) in the lungs of mice; each symbol represents an individual mouse, and lines represent the mean. Data represent pooled results from independent experiments, with n = 6 mice per group per time point, normalized to lung weight. The CFU in the lungs of the phage-treated group showed significant or highly significant reductions at all time points compared with the Mock-treated group.

(D) PFU in the lungs of phage-treated mice. Each symbol represents a logarithmic value, and lines represent the mean. Results represent pooled data from independent experiments, with n = 6 mice per time point, normalized to lung weight.Significant differences in PFU in the lungs were observed at the end of mouse treatment (168 h) and at other time points (12 h, 24 h, and 48 h).

(E) TNF-α levels in mouse lungs; n = 6 mice per group per time point, with two replicates per mouse. Lines represent the mean. Significant differences in TNF-α levels were observed between the Phage-treated and Mock-treated groups at all time points.

(F) Histopathological analysis of lung tissue; scale bar = 100 μm. Survival curves were analyzed using the log-rank test, while other data were analyzed using two-way ANOVA. ***$p < 0.001$, **$p < 0.01$, *$p < 0.05$.

Discussion

The global rise of antimicrobial resistance (AMR) poses a serious public health threat[23, 24]. Phage therapy, recognized for its antibacterial properties[11], offers distinct advantages over conventional treatments, including targeted activity, safety, and without disturbing the commensal microbiota[25]. Recent high-profile clinical

cases and ongoing trials in countries like the U.S., France, and Sweden underscore its potential in combating multidrug-resistant (MDR) pathogens[26].

In this study, we isolated and characterized the bacteriophage vB_AbaS_qsb1, a virulent phage with potent lytic activity against *A.baumannii*. vB_AbaS_qsb1 demonstrated remarkable stability across a broad temperature (10-60□) and pH range (pH 3-11), indicating its potential for use under diverse physiological conditions. The phage's short latent period allows rapid bacterial lysis, despite its moderate burst size. These findings will support vB_AbaS_qsb1 as a promising candidate for therapeutic infection of *A.baumannii*.

Genomic analysis of vB_AbaS_qsb1 classified it within the Caudoviricetes family, supporting its designation as the founding member of a novel genus, which we propose to name *Acinibactriovirus*, with *Acinibactriovirus lysinus* as the type species. Although vB_AbaS_qsb1 harbors an integrase gene (CDS_1) often associated with lysogeny, both experimental data and lifestyle prediction analyses confirmed that it exhibits characteristics of a virulent phage. This integrase gene offers an interesting avenue for further study in phage-host interactions and gene-editing applications.

The genome of vB_AbaS_qsb1 also encodes a lysozyme (CDS_6), likely enhancing its capability to degrade extracellular polysaccharides, positioning this phage as a potential anti-biofilm and anti-infective tool[27]-[28]. Intriguingly, qsb1 produced a prominent depolymerase halo during bacterial lysis, though no specific depolymerase gene was detected, suggesting that its depolymerase function may arise from "viral dark matter"—genes that remain uncharacterized.

Our findings thus establish vB_AbaS_qsb1 as the prototype of the newly proposed *Acinibactriovirus* genus, highlighting its distinct genomic features and promising therapeutic potential.

Safety is a critical factor in the clinical use of phage therapy[27]. In this study, intratracheal administration of 10□ PFU vB_AbaS_qsb1 to mice did not induce adverse clinical symptoms, with stable inflammatory markers and no significant lung tissue damage. These results confirm the safety of vB_AbaS_qsb1, essential for its clinical advancement. Moreover, further in vivo experiments demonstrated its therapeutic efficacy, phage significantly reducing bacterial loads of lung and improving survival rates in mice with *A.baumannii* lung infections. The phages persisted in the lungs for up to a week post-treatment without immune system clearance, continuously reducing bacterial load while proliferating. This, combined with their host specificity and minimal impact on beneficial microbiota, highlights their potential as an effective alternative against multidrug-resistant bacterial infections.

While our results are promising, several limitations remain. The efficacy of vB_AbaS_qsb1 in chronic infections hosts warrants further study. Additionally, the survival rate of treated mice, although improved, remained at 50%. This may be attributed to mechanical damage during phage administration or the empirical nature of current phage therapy protocols[29, 30]. Therefore, future studies can further evaluate the impact of different administration routes of phage on the survival rate of mice while ensuring safety. Finally, in addition to the route of administration, it is

worth further study on whether to use a single phage or a phage cocktail, phage dosage and endotoxin levels in phage preparations, frequency and time of administration, and phage neutralizing antibodies.

In conclusion, we successfully isolated and characterized a novel *A.baumannii* virulent phage, vB_AbaS_qsb1. This phage exhibited potent lytic activity both in vitro and in vivo, demonstrating its ability to effectively eliminate *A.baumannii*, highlighting its potential as a promising therapeutic agent. Additionally, this phage exhibited a favorable safety profile in animal models, with treatment using qsb1 rescuing over 50% of mice with acute *A.baumannii* pneumonia. Notably, qsb1 maintained high phage titers in the lungs 7 days post-administration, which may also indicate that qsb1 has certain potential in the preventive treatment of *A.baumannii* infection. As antibiotic resistance continues to rise, phage therapy holds great promise as an alternative or adjunct to traditional antimicrobial treatments.

Material and method

Bacterial strains and culture conditions

A.baumannii ioag01 was obtained from our laboratory in a previous study[31]. In this study, *ioag01* was used as a host strain to isolate phages. The frozen bacteria were first streaked on Luria-Bertani Broth for 12 h (37 □), and then single colonies were picked and enriched in liquid culture medium in a constant temperature shaking incubator at 220 rpm (37 □, 12 h). The bacterial culture was stored at -80 □ for long-term with 10% glycerol as a cryoprotectant.

Phage isolation and purification

Water samples were collected from the lake in Qishan Lake Park, Fuzhou City, Fujian Province, China. The samples were centrifuged and filtered through a 0.22 μm PES membrane filter. The filtrate was collected in a sterile centrifuge tube. For the enrichment of bacteriophages, the bacterial culture (*A.baumannii ioag01*) was first centrifuged and the supernatant was removed. The bacterial precipitate was resuspended in the 2× LB liquid medium and an equal volume of filtrate was added to it. The mixture was co-cultured at 220 rpm (37 □, 5~7 d). The mixture solution was then centrifuged at 20,000 g (4 □, 10 min). The supernatant was collected and the presence of phages was detected by the drop method[32].For positive samples detected by the drop method, the phage suspension was first serially diluted using SM buffer (1.972 g/L $MgSO_4 \cdot 7H_2O$, 5.85 g/L NaCl, 50 mL/L 1M Tris-HCl（pH 7.5）, 5.0 mL/L 2% Gelatin). Subsequently, 500 μL of the phage dilution was mixed with 500 μL of bacterial culture and incubated at 37 □ for 10 minutes. The 1 mL mixture was then added to 0.6% semi-solid medium and layered onto the surface of a 1.5% solid medium to form double-layer plates, which were incubated overnight at 37 □. Individual plaques were picked into SM buffer on the second day. To purify the isolated phage, an individual plaque was picked and passaged at 3~5 times by the double-layer agar (DLA) method. Single plaques were collected to complete the purification and determine the phage titer.

Phage amplification, concentration, and storage

A 500 μL aliquot of the purified phage lysate was mixed with 500 μL of bacterial culture and incubated overnight at 37 □. The mixture was then centrifuged at 20,000

g (4 □, 10 min). The phage-containing supernatant was collected and added to 5 mL of bacterial culture. This mixture was incubated at 220 rpm (37 □) until the culture became clear. Subsequently, the culture was centrifuged again at 20,000 g (4 □, 10 min). The supernatant was filtered through a 0.22 μm PES membrane to obtain the phage suspension. The phage suspension was then mixed with a 4× virus concentration solution (400 g/L PEG-8000, 70 g/L NaCl, 100 mL/L 10× PBS buffer, pH 6.8) at a 3:1 (v/v) ratio and allowed to stand at 4 □ overnight. Following this, the mixture was centrifuged at 12,000 g (4 □, 15 min), and the supernatant was discarded. The phage pellet was resuspended in SM buffer. Finally, the phage particles were stored at -80 □ using 10 mg/mL PEG-4000 as a cryoprotectant for long-term preservation.

Transmission electron microscopy (TEM)

A 20 μL aliquot of the concentrated phage particle suspension was applied to the surface of a carbon-coated copper grid and allowed to stand for 10 minutes. Excess liquid was then removed using filter paper. The grid was subsequently stained with 20 μL of 2% phosphotungstic acid for 90 seconds to achieve negative staining. After removing the excess stain with filter paper, the grid was left to dry overnight. Imaging was performed using a transmission electron microscope (TEM, HT7800, HITACHI) operating at an accelerating voltage of 100 kV.

Multiplicity of infection (MOI) of phages

The concentration of the host bacterial culture was determined by turbidimetry, and the bacterial concentration was adjusted to 10^8 CFU/mL. The titer of phage qsb1 was

then determined using the DLA method. Phage and host bacterial cultures were mixed in equal volumes at MOI of 0.01, 0.1, 1, 10, and 100, and incubated with shaking at 220 rpm (37 □, 6 h). Following incubation, the cultures were centrifuged, and the phage titer was measured. Three independent experiments were performed.

One-Step growth curve of phages

The phage and host bacterial culture were mixed at the optimal multiplicity of infection (MOI=0.1) determined previously, and incubated at 37 □ for 10 minutes. The supernatant was then discarded, and the precipitate was washed once with LB liquid medium by centrifugation at 20,000 g (4 □, 1 min). The precipitate was resuspended in LB medium and incubated with shaking at 220 rpm (37 □, 4h). Samples were collected every 20 minutes during the first 2 hours, and every 30 minutes during the final 2 hours, for phage titer determination. Three independent experiments were performed.

Temperature and pH stability of phages

To assess the temperature stability of phage qsb1, a phage suspension with a previously measured titer was incubated at temperatures of 10 □, 20 □, 40 □, 60 □, 80 □, and 100 □ for 30, 60, and 90 minutes, respectively, followed by phage titer determination. Three independent experiments were performed.

Similarly, to evaluate the pH stability of phage qsb1, 100 μL of phage suspension (with a known titer) was mixed with 900 μL of SM buffer at various pH levels (1, 3, 5, 7, 8, 9, 11, 13) and incubated (4 □,1 h). Subsequently, the pH of the mixtures was adjusted with appropriate amounts of NaOH or HCl to a level suitable for bacterial

growth, and the phage titer was measured. Three independent experiments were performed.

Extraction, sequencing, and analysis of phage genomes

The total genome of the phage was extracted using the phenol-chloroform method, with nuclease digestion performed beforehand to eliminate host bacterial nucleic acids from the sample. The concentration of the extracted genome was measured using a Nanodrop 2000 spectrophotometer (Thermo Fisher Scientific). The genome was treated with RNase A (Gproan, GPE007001), DNase I (Thermo Fisher Scientific, EN0521), and S1 nucleases (Thermo Fisher Scientific, EN0321) to confirm its nucleic acid type and structural integrity. Subsequently, Pulsed-Field Gel Electrophoresis(Pippin-pluse，sage science) was employed to confirm the size of the phage genome nucleic acid.Next-generation sequencing (NGS) library of the phage genome was constructed using the Nextera library preparation kit, followed by high-throughput sequencing on the Illumina NovaSeq™ X Plus system.

Post-sequencing, quality control of the raw data was conducted to ensure high-quality reads, which were then assembled using MEGAHIT software[33]. For functional annotation of the assembled phage sequences, several bioinformatics tools were utilized, including Prokka[34],RAST[35], GeneMarks[36], Phagescope[37],and Phastest[38]. Phage lifestyle prediction was conducted using the DeepPhage[39] tool to determine whether the isolated phage exhibits a lytic or lysogenic lifecycle.The integrated gene annotation results provided comprehensive genomic information for the phage qsb1.Genomic features were visualized using the CGView[40] online

server.

Phylogenetic analysis

The phage genome was compared with the virus database in the NCBI database by BLAST (using the nt_Viruses datebase and algorithm of Highly similar sequences (megablast)), and then the genomes of *Acinetobacter* phages with full genome sequences in the comparison results were downloaded (74 of 88 sequences) for phylogenetic tree construction.Phylogenetic trees and clustering of phage genomes were constructed using VICTOR[41],which based on a Genome BLAST Distance Phylogeny (GBDP) to obtain a more accurate taxonomic classification. Average nucleotide identity (ANI) analysis was performed using the ANI Calculator[42]. Average amino acid identity (AAI) analysis was carried out based on a pairwise comparison of *Acinetobacter* phage sequences using CompareM (https://github.com/dparks1134/CompareM) with default parameters. For comparative analysis of whole-genome collinearity among phages, RStudio[43] with the gggenomes package[44] was employed to generate a whole-genome comparison visualization map.

Mice

For all mouse experiments, we selected male BALB/C mice aged 6-8 weeks. Upon arrival at the facility, the mice randomly were housed in clean individually ventilated cages (IVC) with 5-6 mice per group, Random numbers were generated using the standard = RAND() function in Microsoft Excel. All mice were used after a 7-day acclimatization period. They were fed with irradiated sterilized feed and provided

distilled water sterilized by high-pressure wet heat. The housing conditions were maintained at a constant temperature of 24-26 □, humidity of 50%-60%, with a 12-hour light/dark cycle.

Preparation of bacterial culture and phage suspension

The bacterial culture of *A.baumannii* was prepared as described in section 2.1, with the concentration adjusted by turbidimetry. A 1 mL aliquot of the bacterial culture was centrifuged at 20,000 g (4 □, 10 min), and the pellet was collected. The pellet was washed with 0.9% NaCl, and then resuspended in 30 μL of 0.9% NaCl for use. Bacteria were removed from the phage suspension using a 0.22 μm microporous membrane, and the phage titer was subsequently determined using the DLA method. Subsequently, the phage suspension was centrifuged at 100,000 g (4 □, 2 h). The phage pellet was resuspended in 0.9% NaCl to a final concentration of 1×10^{12} PFU/mL for further use.

Establishment of a mouse pneumonia model via intratracheal instillation

In previous studies, tracheal access often involved surgical procedures to locate the trachea for drug administration or model establishment, which could introduce experimental variability, such as post-surgical infections or complications during the procedure. To mitigate these risks, we employed a Non-invasive intratracheal instillation approach to construct the mouse pneumonia model [45]. This method is straightforward, rapid, and effective. The anesthetized mouse was positioned supine on an intubation platform, with the head secured, and a disposable indwelling needle was inserted into the glottis using a small animal laryngoscope to complete the

endotracheal intubation.

The model of pulmonary infection caused by *A.baumannii* in mice and phage safety

To induce neutropenia and simulate the immunocompromised state of clinical patients, mice were intraperitoneally injected with cyclophosphamide(CTX) at doses of 200 mg/kg and 150 mg/kg, 4 days and 1 day prior to infection, respectively. In previous studies, a bacterial dose ranging from 10□ ~ 10□ CFU was commonly used to establish an acute pulmonary bacterial infection model in mice[46]. In this study, mice were anesthetized and inoculated via tracheal instillation with varying doses of *A.baumannii ioag01* (3×10□ CFU/mouse, 3×10□ CFU/mouse, 3×10□ CFU/mouse, 3×10□ CFU/mouse). In the phage-treated group, mice were administered 1×10□ PFU/mouse of phage qsb1 via tracheal instillation, while the control group received an equivalent volume of 0.9% NaCl. Mice were observed for seven days, and survival rates were recorded to determine the median lethal dose (LD50) of the bacteria and to evaluate the safety of the phage treatment.

Phage treatment for acute pulmonary infection caused by *A.baumannii* in mice

After determining the appropriate bacterial dose (3×10^8 CFU/mouse) for the mouse lung infection model, phages were used to treat the infected mice to assess therapeutic efficacy. Twenty-five BALB/C mice were randomly divided into five groups. They were intraperitoneally injected with 200 mg/kg and 150 mg/kg of CTX, 4 days and 1 day before infection, respectively. Mice were anesthetized and infected with 3×10^8 CFU of *A.baumannii ioag01*. One hour post-infection, 30 μL of 0.9% NaCl was

administered by tracheal instillation (mock-treated group). The experimental groups received varying phage titers (3×10^9 PFU, high-dose; 3×10^8 PFU, medium-dose; and 3×10^7 PFU, low-dose). The control group received 30 μL of 0.9% NaCl initially, and an additional 30 μL of 0.9% NaCl one hour later to control for procedural variables. All mice were observed for seven days, during which their conditions and mortality were recorded.

High-Dose phage treatment for acute pulmonary infection caused by *A.baumannii* in mice

To further evaluate the pathological changes during infection and the therapeutic effect of high-dose phage treatment, 48 BALB/C mice were randomly divided into two groups. They were injected intraperitoneally with 200 mg/kg and 150 mg/kg of CTX, 4 days and 1 day prior to infection, respectively. After anesthesia, a lung infection model was established as previously described. One hour after bacterial infection, the experimental group received 3×10^9 PFU of phage by tracheal instillation, while the control group received 30 μL of 0.9% NaCl. Subsequently, six mice were euthanized by cervical dislocation at 12、24、48 and 168 hours post-infection. Whole blood and lung tissues were collected aseptically from each mouse. Whole blood and lung tissues were collected under sterile conditions. CBC were conducted to evaluate systemic responses, while bacterial and phage colonization in the lungs was assessed by homogenizing the right lung. The left lung was fixed in paraformaldehyde and stained with hematoxylin-eosin (HE) to assess lung pathology.

Statistical analysis.

Data were evaluated using two-way ANOVA or the log-rank test for survival curves, unless otherwise indicated. A p-value of ≤0.05 was considered statistically significant.

Transparency declaration

Conflict of interest

The bacteriophage strain vB_AbaS_qsb1 has been filed for a patent.

Funding

This work was supported by the Fujian Provincial Department of Science and Technology (No. 2024J011223); Fuzhou Municipal Health Commission (No. 2022-S-wr4) and (No. 2022-S-rc5); Ministry of Science and Technology of the People's Republic of China (No. 2023YFC3304304); Fuzhou University (No. 2024T021); Fujian Provincial Department of Science and Technology (No. 2022Y4003) and (No. 2022ZD01001);

Data availability

The datasets generated during and/or analyzed during the current study are available from the corresponding author on reasonable request. All other data supporting the findings of this study are included within the article and its supplementary materials. (The NGS raw sequencing data have been deposited in the SRA databases, SRA data accession: PRJNA1170883)

CRediT authorship contributions statement

JiaWang.Wang: Data curation, Formal analysis, Investigation, Validation, Visualization, Writing – original draft; **Huan.Hu:** Funding acquisition, Investigation, Software; **QingQing.Wang:**

Investigation; **TianZhu.Zhu:** Software, Validation, Visualization; **XiaoHan.Ren:** Software, Visualization; **WenQian.Jiang:** Investigation; **XueMei.Hou:** Investigation, Project administration, Supervision, Writing – review and editing; **Jun.Lin:** Conceptualization, Funding acquisition, Methodology, Project administration, Resources, Supervision, Writing – review and editing; **XiaoLing.Yu:** Conceptualization, Funding acquisition, Methodology, Project administration, Resources, Supervision, Writing – review and editing

Ethical statement

All protocols in this study were approved by the Committee on the Ethics of Animal Experiments of College of Biological Science and Engineering, Fuzhou University (the authority of the project licence: KS2023-SG-042)

Declaration of Generative AI and AI-assisted technologies in the writing process

During the preparation of this work the author(s) used Chat-GPT 4o in order to improve the language and readability,with caution. After using this tool, the authors reviewed and edited the content as needed and take full responsibility for the content of the publication.

Reference

1. Bianco A, Quirino A, Giordano M, Marano V, Rizzo C, Liberto MC, et al. Control of carbapenem-resistant Acinetobacter baumannii outbreak in an intensive care unit of a teaching hospital in Southern Italy. BMC Infect Dis. 2016;16(1):747. Epub 20161212. doi: 10.1186/s12879-016-2036-7. PubMed PMID: 27955639; PubMed Central PMCID: PMCPMC5154034.

2. Ayoub Moubareck C, Hammoudi Halat D. Insights into Acinetobacter baumannii: A Review of Microbiological, Virulence, and Resistance Traits in a Threatening Nosocomial Pathogen. Antibiotics

(Basel). 2020;9(3). Epub 20200312. doi: 10.3390/antibiotics9030119. PubMed PMID: 32178356; PubMed Central PMCID: PMCPMC7148516.

3. Hafiz TA, Alghamdi SS, Mubaraki MA, Alghamdi SSM, Alothaybi A, Aldawood E, et al. A two-year retrospective study of multidrug-resistant Acinetobacter baumannii respiratory infections in critically Ill patients: Clinical and microbiological findings. J Infect Public Health. 2023;16(3):313-9. Epub 20230111. doi: 10.1016/j.jiph.2023.01.004. PubMed PMID: 36641839.

4. Mohd Sazlly Lim S, Zainal Abidin A, Liew SM, Roberts JA, Sime FB. The global prevalence of multidrug-resistance among Acinetobacter baumannii causing hospital-acquired and ventilator-associated pneumonia and its associated mortality: A systematic review and meta-analysis. J Infect. 2019;79(6):593-600. Epub 20190930. doi: 10.1016/j.jinf.2019.09.012. PubMed PMID: 31580871.

5. Mulani MS, Kamble EE, Kumkar SN, Tawre MS, Pardesi KR. Emerging Strategies to Combat ESKAPE Pathogens in the Era of Antimicrobial Resistance: A Review. Front Microbiol. 2019;10:539. Epub 20190401. doi: 10.3389/fmicb.2019.00539. PubMed PMID: 30988669; PubMed Central PMCID: PMCPMC6452778.

6. Vestergaard M, Paulander W, Marvig RL, Clasen J, Jochumsen N, Molin S, et al. Antibiotic combination therapy can select for broad-spectrum multidrug resistance in Pseudomonas aeruginosa. Int J Antimicrob Agents. 2016;47(1):48-55. Epub 20151025. doi: 10.1016/j.ijantimicag.2015.09.014. PubMed PMID: 26597931.

7. Clark NM, Zhanel GG, Lynch JP, 3rd. Emergence of antimicrobial resistance among Acinetobacter species: a global threat. Curr Opin Crit Care. 2016;22(5):491-9. doi: 10.1097/MCC.0000000000000337. PubMed PMID: 27552304.

8. Gallagher P, Baker S. Developing new therapeutic approaches for treating infections caused by multi-drug resistant Acinetobacter baumannii: Acinetobacter baumannii therapeutics. J Infect. 2020;81(6):857-61. Epub 20201025. doi: 10.1016/j.jinf.2020.10.016. PubMed PMID: 33115656.

9. Organization WH. WHO publishes list of bacteria for which new antibiotics are urgently needed: World Health Organization; 2017 [cited accessed 10 Oct 2024]. Available from: https://www.who.int/news-room/detail/27-02-2017-who-publishes-list-of-bacteria-for-which-new-antibiotics-are-urgently-needed.

10. organization Wh. WHO updates list of drug-resistant bacteria most threatening to human health: World health organization; 2024 [cited accessed 10 Oct 2024]. Available from: https://www.who.int/zh/news/item/17-05-2024-who-updates-list-of-drug-resistant-bacteria-most-threatening-to-human-health.

11. Salmond GP, Fineran PC. A century of the phage: past, present and future. Nat Rev Microbiol. 2015;13(12):777-86. Epub 20151109. doi: 10.1038/nrmicro3564. PubMed PMID: 26548913.

12. Tao P, Gu J, Barr JJ. Editorial: The Application of Phages Against Infectious Diseases. Front Cell Infect Microbiol. 2021;11:815984. Epub 20211220. doi: 10.3389/fcimb.2021.815984. PubMed PMID: 34988033; PubMed Central PMCID: PMCPMC8721092.

13. Jamal M, Andleeb S, Jalil F, Imran M, Nawaz MA, Hussain T, et al. Isolation, characterization and efficacy of phage MJ2 against biofilm forming multi-drug resistant Enterobacter cloacae. Folia Microbiol (Praha). 2019;64(1):101-11. Epub 20180808. doi: 10.1007/s12223-018-0636-x. PubMed PMID: 30090964.

14. Wang Y, Subedi D, Li J, Wu J, Ren J, Xue F, et al. Phage Cocktail Targeting STEC O157:H7 Has Comparable Efficacy and Superior Recovery Compared with Enrofloxacin in an Enteric Murine Model.

Microbiol Spectr. 2022;10(3):e0023222. Epub 20220510. doi: 10.1128/spectrum.00232-22. PubMed PMID: 35536028; PubMed Central PMCID: PMCPMC9241756.

15. Gordillo Altamirano FL, Kostoulias X, Subedi D, Korneev D, Peleg AY, Barr JJ. Phage-antibiotic combination is a superior treatment against Acinetobacter baumannii in a preclinical study. EBioMedicine. 2022;80:104045. Epub 20220507. doi: 10.1016/j.ebiom.2022.104045. PubMed PMID: 35537278; PubMed Central PMCID: PMCPMC9097682.

16. Ashworth EA, Wright RCT, Shears RK, Wong JKL, Hassan A, Hall JPJ, et al. Exploiting lung adaptation and phage steering to clear pan-resistant Pseudomonas aeruginosa infections in vivo. Nat Commun. 2024;15(1):1547. Epub 20240220. doi: 10.1038/s41467-024-45785-z. PubMed PMID: 38378698; PubMed Central PMCID: PMCPMC10879199.

17. Chang RYK, Chow MYT, Wang Y, Liu C, Hong Q, Morales S, et al. The effects of different doses of inhaled bacteriophage therapy for Pseudomonas aeruginosa pulmonary infections in mice. Clin Microbiol Infect. 2022;28(7):983-9. Epub 20220203. doi: 10.1016/j.cmi.2022.01.006. PubMed PMID: 35123053.

18. Nick JA, Dedrick RM, Gray AL, Vladar EK, Smith BE, Freeman KG, et al. Host and pathogen response to bacteriophage engineered against Mycobacterium abscessus lung infection. Cell. 2022;185(11):1860-74 e12. Epub 20220513. doi: 10.1016/j.cell.2022.04.024. PubMed PMID: 35568033; PubMed Central PMCID: PMCPMC9840467.

19. Bernabeu-Gimeno M, Pardo-Freire M, Chan BK, Turner PE, Gil-Brusola A, Perez-Tarazona S, et al. Neutralizing antibodies after nebulized phage therapy in cystic fibrosis patients. Med. 2024. Epub 20240617. doi: 10.1016/j.medj.2024.05.017. PubMed PMID: 38917792.

20. Schooley RT, Biswas B, Gill JJ, Hernandez-Morales A, Lancaster J, Lessor L, et al. Development

and Use of Personalized Bacteriophage-Based Therapeutic Cocktails To Treat a Patient with a Disseminated Resistant Acinetobacter baumannii Infection. Antimicrob Agents Chemother. 2017;61(10). Epub 20170922. doi: 10.1128/AAC.00954-17. PubMed PMID: 28807909; PubMed Central PMCID: PMCPMC5610518.

21. Nir-Paz R, Gelman D, Khouri A, Sisson BM, Fackler J, Alkalay-Oren S, et al. Successful Treatment of Antibiotic-resistant, Poly-microbial Bone Infection With Bacteriophages and Antibiotics Combination. Clin Infect Dis. 2019;69(11):2015-8. doi: 10.1093/cid/ciz222. PubMed PMID: 30869755.

22. Federici S, Kredo-Russo S, Valdes-Mas R, Kviatcovsky D, Weinstock E, Matiuhin Y, et al. Targeted suppression of human IBD-associated gut microbiota commensals by phage consortia for treatment of intestinal inflammation. Cell. 2022;185(16):2879-98 e24. Epub 20220804. doi: 10.1016/j.cell.2022.07.003. PubMed PMID: 35931020.

23. organization Wh. Report signals increasing resistance to antibiotics in bacterial infections in humans and need for better data: World health organization; 2024 [cited accessed 10 Oct 2024]. Available from: https://www.who.int/zh/news/item/09-12-2022-report-signals-increasing-resistance-to-antibiotics-in-bacterial-infections-in-humans-and-need-for-better-data.

24. Murray CJL, Ikuta KS, Sharara F, Swetschinski L, Robles Aguilar G, Gray A, et al. Global burden of bacterial antimicrobial resistance in 2019: a systematic analysis. The Lancet. 2022;399(10325):629-55. doi: 10.1016/s0140-6736(21)02724-0.

25. Ali Y, Inusa I, Sanghvi G, Mandaliya VB, Bishoyi AK. The current status of phage therapy and its advancement towards establishing standard antimicrobials for combating multi drug-resistant bacterial

pathogens. Microbial Pathogenesis. 2023;181. doi: 10.1016/j.micpath.2023.106199.

26. Strathdee SA, Hatfull GF, Mutalik VK, Schooley RT. Phage therapy: From biological mechanisms to future directions. Cell. 2023;186(1):17-31. doi: 10.1016/j.cell.2022.11.017.

27. Li M, Wang H, Chen L, Guo G, Li P, Ma J, et al. Identification of a phage-derived depolymerase specific for KL47 capsule of Klebsiella pneumoniae and its therapeutic potential in mice. Virol Sin. 2022;37(4):538-46. Epub 20220502. doi: 10.1016/j.virs.2022.04.005. PubMed PMID: 35513275; PubMed Central PMCID: PMCPMC9437526.

28. Liu Y, Leung SSY, Huang Y, Guo Y, Jiang N, Li P, et al. Identification of Two Depolymerases From Phage IME205 and Their Antivirulent Functions on K47 Capsule of Klebsiella pneumoniae. Front Microbiol. 2020;11:218. Epub 20200214. doi: 10.3389/fmicb.2020.00218. PubMed PMID: 32117192; PubMed Central PMCID: PMCPMC7034173.

29. Mitropoulou G, Koutsokera A, Csajka C, Blanchon S, Sauty A, Brunet JF, et al. Phage therapy for pulmonary infections: lessons from clinical experiences and key considerations. Eur Respir Rev. 2022;31(166). Epub 20221005. doi: 10.1183/16000617.0121-2022. PubMed PMID: 36198417; PubMed Central PMCID: PMCPMC9724797.

30. Hong Q, Chang RYK, Assafiri O, Morales S, Chan HK. Optimizing in vitro phage-ciprofloxacin combination formulation for respiratory therapy of multi-drug resistant Pseudomonas aeruginosa infections. Int J Pharm. 2024;652:123853. Epub 20240126. doi: 10.1016/j.ijpharm.2024.123853. PubMed PMID: 38280500.

31. Lin J, Jiang W, Shi Y, Cai W. Metagenomic Sequencing Revealed the Potential Pathogenic Threats of Banknotes. ACS Omega. 2021;6(5):3499-507. Epub 20210127. doi: 10.1021/acsomega.0c04546. PubMed PMID: 33585735; PubMed Central PMCID: PMCPMC7876676.

32. Acs N, Gambino M, Brondsted L. Bacteriophage Enumeration and Detection Methods. Front Microbiol. 2020;11:594868. Epub 20201023. doi: 10.3389/fmicb.2020.594868. PubMed PMID: 33193274; PubMed Central PMCID: PMCPMC7644846.

33. Li D, Liu C-M, Luo R, Sadakane K, Lam T-W. MEGAHIT: an ultra-fast single-node solution for large and complex metagenomics assembly via succinct de Bruijn graph. Bioinformatics. 2015;31(10):1674-6. doi: 10.1093/bioinformatics/btv033.

34. Seemann T. Prokka: rapid prokaryotic genome annotation. Bioinformatics. 2014;30(14):2068-9. doi: 10.1093/bioinformatics/btu153.

35. Aziz RK, Bartels D, Best AA, DeJongh M, Disz T, Edwards RA, et al. The RAST Server: Rapid Annotations using Subsystems Technology. BMC Genomics. 2008;9(1). doi: 10.1186/1471-2164-9-75.

36. Besemer J. GeneMarkS: a self-training method for prediction of gene starts in microbial genomes. Implications for finding sequence motifs in regulatory regions. Nucleic Acids Research. 2001;29(12):2607-18. doi: 10.1093/nar/29.12.2607.

37. Wang RH, Yang S, Liu Z, Zhang Y, Wang X, Xu Z, et al. PhageScope: a well-annotated bacteriophage database with automatic analyses and visualizations. Nucleic Acids Res. 2024;52(D1):D756-D61. doi: 10.1093/nar/gkad979. PubMed PMID: 37904614; PubMed Central PMCID: PMCPMC10767790.

38. Wishart DS, Han S, Saha S, Oler E, Peters H, Grant JR, et al. PHASTEST: faster than PHASTER, better than PHAST. Nucleic Acids Res. 2023;51(W1):W443-W50. doi: 10.1093/nar/gkad382. PubMed PMID: 37194694; PubMed Central PMCID: PMCPMC10320120.

39. Wu S, Fang Z, Tan J, Li M, Wang C, Guo Q, et al. DeePhage: distinguishing virulent and temperate phage-derived sequences in metavirome data with a deep learning approach. GigaScience.

2021;10(9). doi: 10.1093/gigascience/giab056.

40. Grant JR, Enns E, Marinier E, Mandal A, Herman EK, Chen CY, et al. Proksee: in-depth characterization and visualization of bacterial genomes. Nucleic Acids Res. 2023;51(W1):W484-W92. doi: 10.1093/nar/gkad326. PubMed PMID: 37140037; PubMed Central PMCID: PMCPMC10320063.

41. Meier-Kolthoff JP, Goker M. VICTOR: genome-based phylogeny and classification of prokaryotic viruses. Bioinformatics. 2017;33(21):3396-404. doi: 10.1093/bioinformatics/btx440. PubMed PMID: 29036289; PubMed Central PMCID: PMCPMC5860169.

42. Yoon SH, Ha SM, Lim J, Kwon S, Chun J. A large-scale evaluation of algorithms to calculate average nucleotide identity. Antonie Van Leeuwenhoek. 2017;110(10):1281-6. Epub 20170215. doi: 10.1007/s10482-017-0844-4. PubMed PMID: 28204908.

43. Team R. RStudio: Integrated Development for R V2024.04.2+764 (version 2024.04.2+764) 2020. Available from: http://www.rstudio.com/.

44. T H, M A, B vA. gggenomes: A Grammar of Graphics for Comparative Genomics.R package (version 1.0.1) 2024. Available from: https://github.com/thackl/gggenomes.

45. Zeng Y, Jin H, Wang J, Guo C, Chen W, Tan Y, et al. An optimized method for intratracheal instillation in mice. J Pharmacol Toxicol Methods. 2022;118:107230. Epub 20221030. doi: 10.1016/j.vascn.2022.107230. PubMed PMID: 36323359.

46. Yang X, Haque A, Matsuzaki S, Matsumoto T, Nakamura S. The Efficacy of Phage Therapy in a Murine Model of Pseudomonas aeruginosa Pneumonia and Sepsis. Front Microbiol. 2021;12:682255. Epub 20210705. doi: 10.3389/fmicb.2021.682255. PubMed PMID: 34290683; PubMed Central PMCID: PMCPMC8287650.

Figure 1

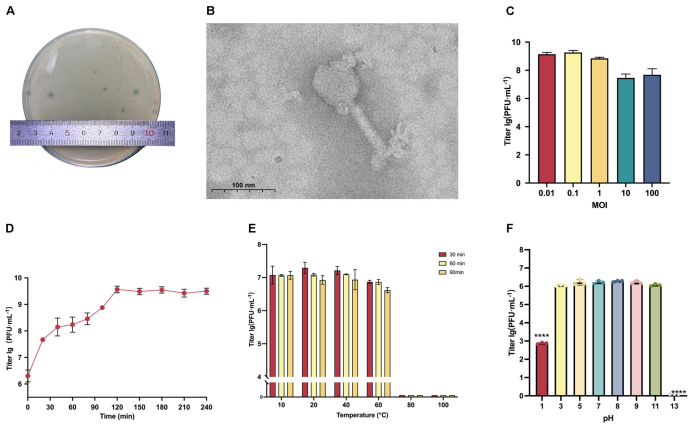

Figure 2

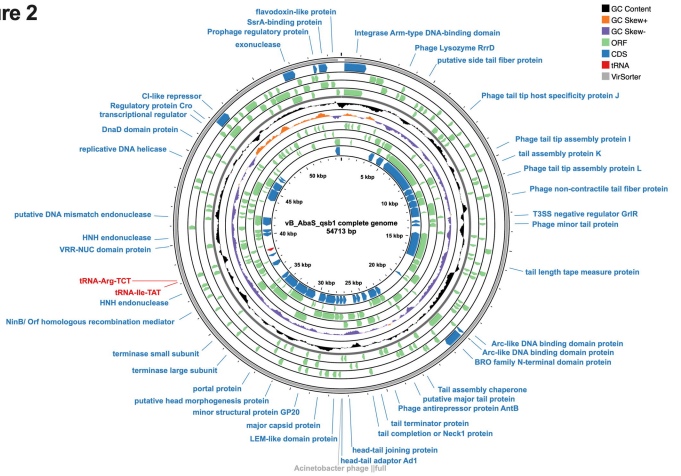

Figure 3

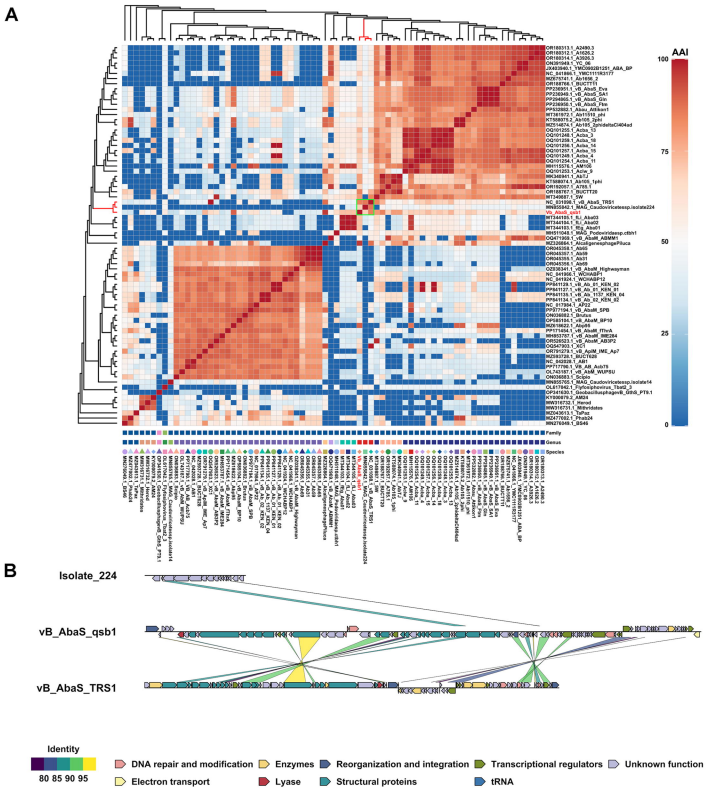

Figure 4

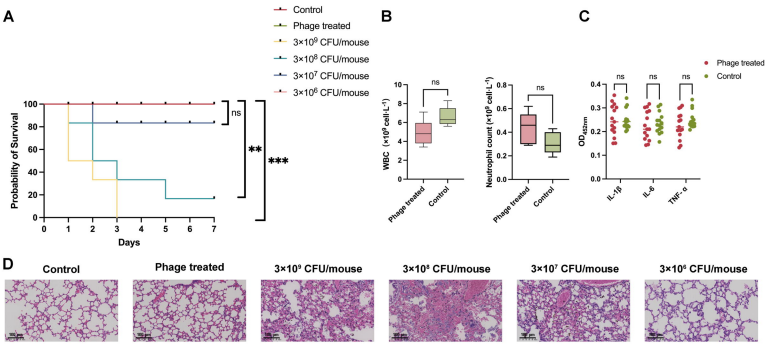

Figure 5

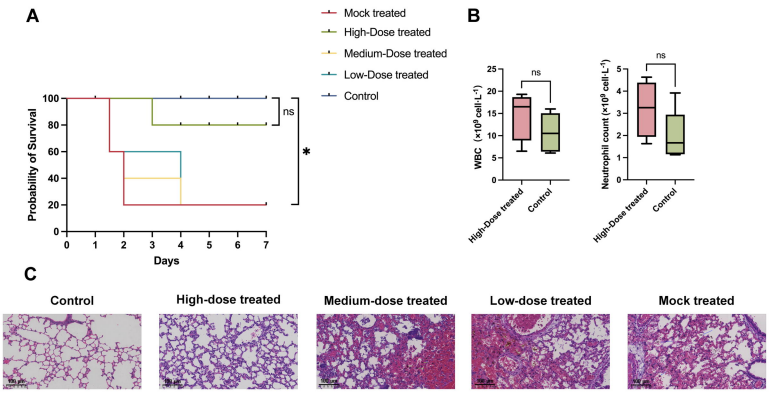
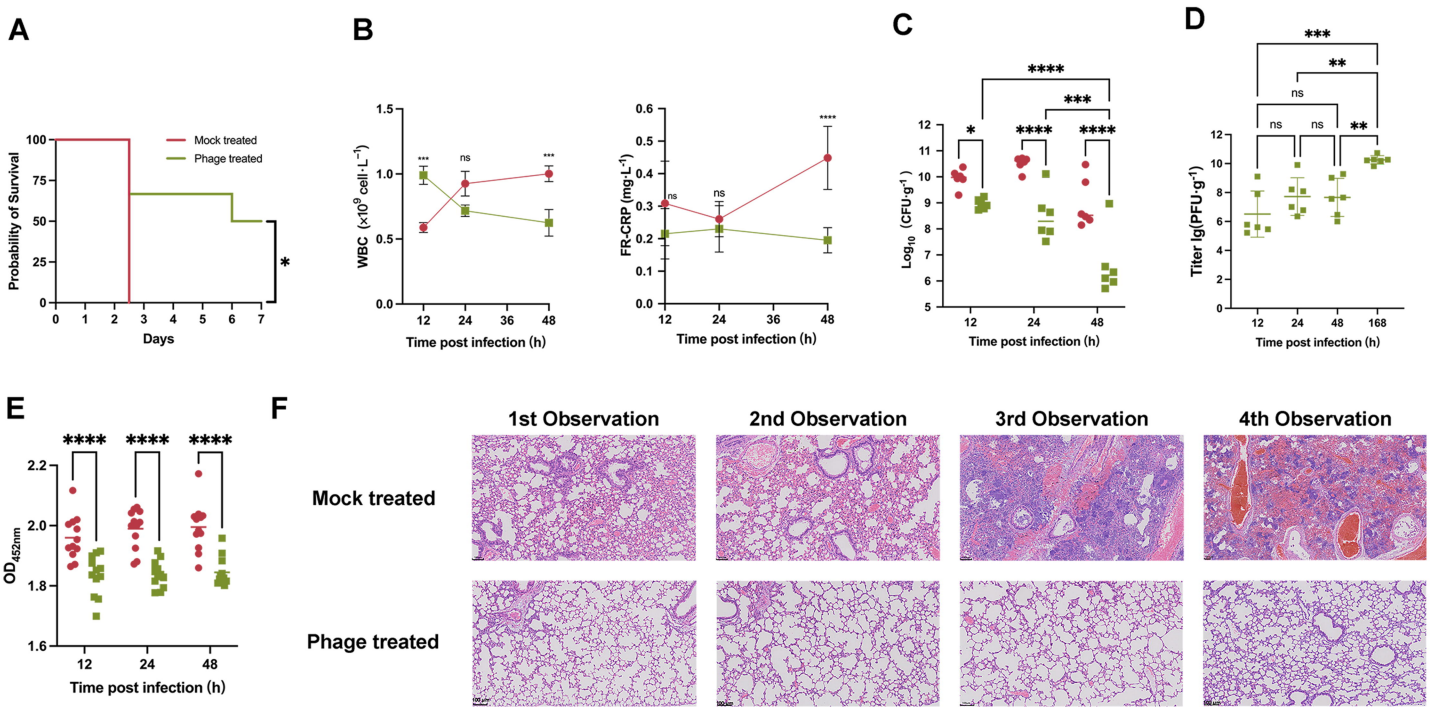
Figure 6